JOURNAL OF GEOPHYSICAL RESEARCH, VOL. 115, C06009, doi:10.1029/2009JC005985, 2010

Refinements to a prognostic scheme of skin sea surface temperature

Yuhei Takaya,[1,2] Jean-Raymond Bidlot,[1] Anton C. M. Beljaars,[1] and Peter A. E. M. Janssen[1]

Received 13 November 2009; revised 20 January 2010; accepted 4 February 2010; published 15 June 2010.

[1] Refinements to a prognostic scheme of skin sea surface temperature (SST) are proposed and tested. The refinements consist of two modifications of a Monin-Obukhov similarity function for stable conditions and mixing enhancement by the Langmuir circulation. The modified scheme is tested with the European Centre for Medium-Range Weather Forecasts model. The modified scheme shows better agreement of the diurnal SST amplitude with estimates from satellite observations. The scheme is also validated with moored buoy observations of the Arabian Sea Mixed Layer Dynamics Experiment. The off-line model with the modified scheme reproduces the observed diurnal SST variability well. Additionally, it is found that the parameterization of the effect of the Langmuir circulation enhances ocean mixing and reduces the diurnal variability of SST under wavy conditions.

Citation: Takaya, Y., J.-R. Bidlot, A. C. M. Beljaars, and P. A. E. M. Janssen (2010), Refinements to a prognostic scheme of skin sea surface temperature, *J. Geophys. Res.*, *115*, C06009, doi:10.1029/2009JC005985.

1. Introduction

[2] Sea surface temperature is an important parameter for atmosphere-ocean interaction. Traditionally sea surface temperature (SST) has been analyzed as so-called bulk SST, which is temperature analyzed from various types of observations at about 1 m or deeper [*Donlon et al.*, 2007]. Meanwhile, satellite observations and shipboard radiometric measurements show that skin SST [*Donlon et al.*, 2007] has diurnal variability of up to a few degrees in low wind and clear sky conditions [e.g., *Gentemann et al.*, 2003; *Gentemann and Minnett*, 2008]. The diurnal variability of skin SST has a direct influence on surface fluxes and the atmospheric variability from diurnal to intraseasonal time scales [e.g., *Kawai and Wada*, 2007; *Webster et al.*, 1996]. Therefore simulating accurate skin SST is crucial for improving numerical weather prediction or data assimilation.

[3] For representing the diurnal SST variation, some diagnostic and prognostic models have been developed [*Fairall et al.*, 1996a; *Stuart-Menteth et al.*, 2003; *Webster et al.*, 1996; *Zeng and Beljaars*, 2005, hereafter ZB05]. The ZB05 scheme has been introduced in the operational version of the European Centre for Medium-Range Weather Forecasts (ECMWF) forecast model (CY35R1) in September 2008, and the scheme improved the prediction skill of the Madden-Julian oscillation [*Madden and Julian*, 1994] in medium-range forecasts (F. Vitart, personal communication, 2009). *Brunke et al.* [2008] showed that the ZB05 scheme has a significant impact on the mean climate in the Community Atmosphere Model (CAM3.1).

[4] Although the ZB05 scheme can represent the diurnal SST variation, some deficiencies of the diurnal SST amplitude (DSA) have been reported recently [*Bellenger and Duvel*, 2009]. To remove these deficiencies, we propose two refinements to the ZB05 scheme, namely changes to the stability function in the diffusion and the addition of the Langmuir circulation effect. The modified scheme is evaluated making use of satellite data and buoy observations.

2. Skin SST Scheme

[5] The ZB05 scheme solves the one-dimensional heat transfer equation in the near-surface layer. A cool skin layer is parameterized in the same way as ZB05. So we focus on a warm layer here. The equation for the warm layer is given by

$$\frac{\partial T}{\partial t} = \frac{\partial}{\partial z}\left(K_w \frac{\partial T}{\partial z}\right) + \frac{1}{\rho_w c_w}\frac{\partial R}{\partial z}, \tag{1}$$

where T is temperature and z is the depth defined as positive upward, ρ_w and c_w are the water density and heat capacity, K_w is the turbulent diffusivity and R is the net solar radiation flux. We integrate the equation between the bottom of the cool skin layer ($z = -\delta$) and the depth ($z = -d$) where the diurnal SST variation can be neglected. The result is

$$\frac{\partial}{\partial t}\int_{-d}^{-\delta} T dz = \frac{Q + R(0) - R(-d)}{\rho_w c_w} - K_w \frac{\partial T}{\partial z}\bigg|_{z=-d}, \tag{2}$$

[1]European Centre for Medium-Range Weather Forecasts, Reading, UK.
[2]Japan Meteorological Agency, Tokyo, Japan.

0148-0227/10/2009JC005985

where Q is the net heat flux including the surface latent and sensible heat fluxes and the net longwave radiation flux, defined as positive downward. In this study, d is 3 m as with ZB05. The solar radiation profile $R(z)$ is parameterized by the Soloviev formulation [*Soloviev*, 1982].

[6] To compute the diffusivity, the ZB05 scheme uses a parameterization based on the Monin-Obukhov similarity theory. The diffusivity is expressed as

$$K_w(z) = \frac{-\kappa z u_w^* f(La)}{\phi_h(\zeta)}, \tag{3}$$

where κ = 0.4 is the von Kármán's constant, ϕ_h is the similarity function and $\zeta = -z/L$ is the stability parameter. Following *Large et al.* [1994], the Obukhov length L is given as

$$L = \rho_w c_w u_w^{*3} / (\kappa g \alpha_w (Q + R(0) - R(z))), \tag{4}$$

where g is gravity, α_w is the thermal expansion coefficient. The friction velocity is $u_w^* = \sqrt{\tau/\rho_w}$ using surface wind stress τ and water density ρ_w. The function $f(La)$ is a function of the Langmuir number to parameterize the effect of the Langmuir circulation. We discuss this function below.

[7] Recent observational studies of a flux-profile relationship have pointed out that the similarity function $\phi_h(\zeta)$ (the nondimensional temperature gradient) in strongly stable conditions levels off and approaches to a constant as ζ increases [*Cheng and Brutsaert*, 2005; *Grachev et al.*, 2007]. In the ocean, the near-surface layer is strongly stable under calm and clear sky conditions, because the water density is $O(10^3)$ larger than the air density. The larger density gives smaller u_w^* and L, and larger ζ. Measurements of turbulent fluxes under strongly stable conditions ($\zeta > 1$) are limited and still have large uncertainty [*Cheng and Brutsaert*, 2005; *Grachev et al.*, 2007]. In this study, the similarity function for stable conditions is based on a function obtained from the Surface Heat Budget of the Arctic Ocean Experiment (SHEBA) [*Grachev et al.*, 2007], but we modify its form for strongly stable conditions. The similarity function used in this study is given as

$$\phi_h(\zeta) = \begin{cases} 1 + \dfrac{5\zeta + 4\zeta^2}{1 + 3\zeta + 0.25\zeta^2} & (\zeta \geq 0) \\ (1 - 16\zeta)^{-1/2} & (\zeta < 0), \end{cases} \tag{5}$$

compared to $\phi_h(\zeta) = 1 + 5\zeta$ ($\zeta \geq 0$) from ZB05. For the range between $\zeta = 0$ and $\zeta = 1$, the function used in this study gives a similar curve to the function of *Grachev et al.* [2007].

[8] It has been recognized that ocean surface waves can significantly influence mixing in the upper ocean [*Melville*, 1996; *Sullivan and McWilliams*, 2010; *Thorpe*, 2004]. Ocean waves induce mixing through processes such as the Langmuir circulation [*Langmuir*, 1938] and wave breaking. Enhancement of mixing by ocean surface waves has been confirmed by observations [*Gerbi et al.*, 2008; *Terray et al.*, 1996; *Thorpe et al.*, 2003] and large eddy simulations (LESs) [*Li et al.*, 2005; *McWilliams et al.*, 1997; *Noh et al.*, 2004; *Skyllingstad and Denbo*, 1995; *Sullivan et al.*, 2007]. To parameterize these processes, some studies proposed approaches to include additional wave effects to ocean mixed layer schemes based on the Monin-Obukhov similarity theory [*Gerbi et al.*, 2009; *McWilliams and Sullivan*, 2000; *Smyth et al.*, 2002].

[9] In this study, we include the effect of the Langmuir circulation (the Stokes drift) to the ZB05 scheme following *McWilliams and Sullivan* [2000]. The formulation in this study uses a function of the Langmuir number $La = \sqrt{u_w^*/u_s}$ with the surface Stokes velocity u_s [*McWilliams et al.*, 1997] in order to modify the turbulent velocity scale. The surface Stokes velocity is computed in the ECMWF wave model [*Janssen*, 2004] using a procedure outlined by *Kenyon* [1969]. We apply the velocity scale proposed by *Grant and Belcher* [2009]. The function is given by equation 3 of *Grant and Belcher* [2009] as

$$f(La) = La^{-2/3}. \tag{6}$$

The range of $f(La)$ is limited as $f(La) \geq 1$ so that the Langmuir circulation effect works to enhance ocean mixing [cf. *McWilliams and Sullivan*, 2000]. This function is applied for stable conditions only, because the diffusivity is adjusted to reproduce slow decay of skin SST in the ZB05 scheme.

[10] As with ZB05, assuming that bulk SST is constant, temperature near the surface has a vertical profile as $T = T_{-\delta} - [(z + \delta)/(-d + \delta)]^{\nu} (T_{-\delta} - T_{-d})$ with an empirical parameter $\nu = 0.3$ and assuming $d \gg \delta$, (2) can be written as

$$\frac{\partial}{\partial t}(T_{-\delta} - T_{-d}) = \frac{(\nu + 1)(Q + R(0) - R(-d))}{\nu d \rho_w c_w} - \frac{(\nu + 1)\kappa u_w^* f(La)}{d \phi_h(\zeta)} (T_{-\delta} - T_{-d}). \tag{7}$$

3. Results

3.1. Validation of Diurnal SST Amplitude

[11] To validate the diurnal SST amplitude (DSA), the modified scheme is tested in the ECMWF model (CY35R2) with the resolution of T255L62. Sets of experiments with 10 day forecasts starting from 1 January and July 1990–2007, are used to assess the DSA. The bulk SST, T_{-d} is prescribed using persisted SST anomaly through the integrations. A cool skin layer scheme [ZB05] is also applied in all integrations.

[12] First we verify the DSA with respect to daily averages of 10 m wind speed and shortwave radiation at the surface (insolation). The diagnostic method used in this study is the same as *Bellenger and Duvel* [2009]. The DSA is defined here as a difference between maximum skin SST and minimum skin SST during 00 to 24 local mean time. Hourly outputs between 40°N and 40°S are analyzed. Daily averages of insolation and 10 m wind speed are used to stratify the DSA response. Model results are compared with the DSA estimate from the Tropical Rainfall Measuring Mission (TRMM) Microwave Imager (TMI) SST measurements [*Gentemann et al.*, 2003]. The satellite estimate is obtained together with the shortwave radiation at the top of atmosphere, therefore the value of the shortwave flux at the top of atmosphere (Q in equation 1a of *Gentemann et al.* [2003]) is simply replaced by the surface shortwave flux

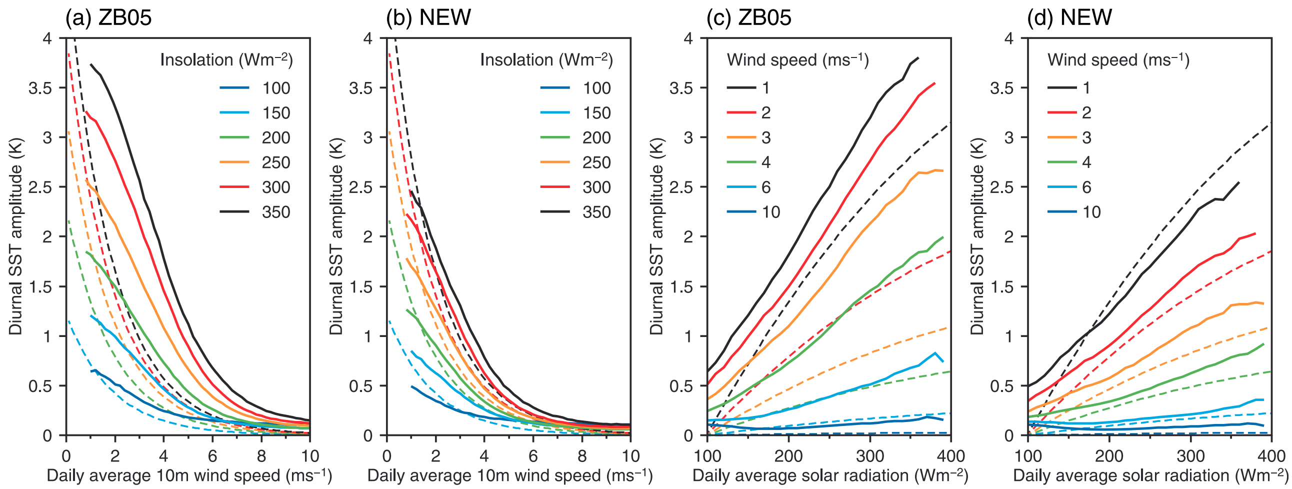

Figure 1. The averaged DSA of (a and c) ZB05 scheme and (b and d) the modified scheme proposed in this study (NEW). The DSA is stratified with daily average surface insolation and 10 m wind speed. The DSA for given daily average insolation with respect to 10 m wind speed (Figures 1a and 1b). The DSA for given daily average 10 m wind speed with respect to insolation (Figures 1c and 1d). Solid (dashed) lines show the model results (satellite estimates [*Gentemann et al.*, 2003]). Bin intervals are 10 W m^{-2} for insolation and 0.2 m s^{-1} for 10 m wind speed. Data is only plotted when a sample size is more than 100.

divided by 0.75 (for further discussion, please see section 3 of *Bellenger and Duvel* [2009]).

[13] Figure 1 shows the DSA stratified with daily averages of insolation and 10 m wind speed. Model results are computed with January and July cases. An overestimation of the DSA in the ZB05 scheme (Figures 1a and 1c) compared with the satellite estimate is consistent with results reported by *Bellenger and Duvel* [2009]. The modified scheme (NEW) shows overall better agreement with the satellite estimate than the ZB05 scheme (Figures 1b and 1d).

[14] Figure 2 shows the spatial distributions of the average DSA computed with January cases. The climatological day-night difference of SST from AMSR-E measurements during 2002–2006 winter [*Kawai and Wada*, 2007] is shown as a reference (Figure 2d). The modified scheme shows a closer DSA to the satellite measurement than the ZB05 scheme (Figures 2a and 2b). It should be noted that some errors of the DSA result from errors of surface heat fluxes and radiation fluxes in the model. The same diagnostic with summer cases shows a similar improvement as shown in Figure 2.

3.2. Impact of the Langmuir Circulation

[15] To investigate the impact of the Langmuir circulation on the DSA, experiments with (NEW) and without the Langmuir circulation effect (noLC) are compared. Figure 3 shows the DSA difference between the two experiments and a reduction ratio of the DSA, which is defined as the DSA difference normalized by the DSA of the experiment without the Langmuir circulation effect. The DSA is stratified with daily average insolation. The reduction of the DSA is about a few tenth of a degree. The reduction ratio shows more than 30% reduction of the DSA in clear sky and moderate wind (5–9 m s^{-1}) conditions. In the ocean, the Langmuir circulation is well developed ($La \sim 0.3$) in moderate and high wind conditions. The modified scheme represents enhanced mixing by the Langmuir circulation and reduces the DSA in these conditions.

[16] Ocean wave conditions depend on basins and seasons. Figure 4 shows the spatial distribution of the averaged Langmuir number computed from integrations started from 1 January 1990–2007. Ocean mixing in regions with the small Langmuir number is dominated by the Langmuir circulation regime [*Li et al.*, 2005], which efficiently damps the DSA (Figures 2b and 2c).

3.3. Off-Line Simulation With Buoy Observations

[17] Off-line simulations with the skin layer schemes are performed and validated with buoy observations of the Arabian Sea Mixed Layer Dynamics Experiment at 15° 30′N, 61° 30′E during a 3 month period from March to May 1995 [*Baumgartner et al.*, 1997, *Weller et al.*, 2002]. The diurnal warming of skin SST is profound in the Arabian Sea in spring [see *Kawai and Wada*, 2007, Figure 5]. The off-line skin layer model is driven by hourly surface fluxes computed with the COARE flux algorithm [*Fairall et al.*, 1996b] using Improved Meteorology (IMET) buoy observations. The buoy temperature observation and surface flux data were downloaded from the Web page of the Woods Hole Oceanographic Institution (http://uop.whoi.edu/archives/arabiansea/arabiansea.html). For this verification, temperature measurements at a depth of 0.17 m from the WHOI buoy are used. The cool skin scheme is deactivated in order to compare with the temperature observation at 0.17 m. Observed temperature at a depth of 3.5 m is prescribed as the bulk temperature T_{-d}. The Stokes drift velocity is computed from the ERA-Interim wave analysis [*Simmons et al.*, 2007]. The 6 hourly Stokes drift velocity is interpolated in time and supplied for the modified skin layer scheme.

[18] Since in situ radiometric measurements of skin SST are unavailable for this experiment, only an indirect verification of the skin SST is possible. In very calm and clear sky conditions, the temperature profiles within the upper 0.5 m

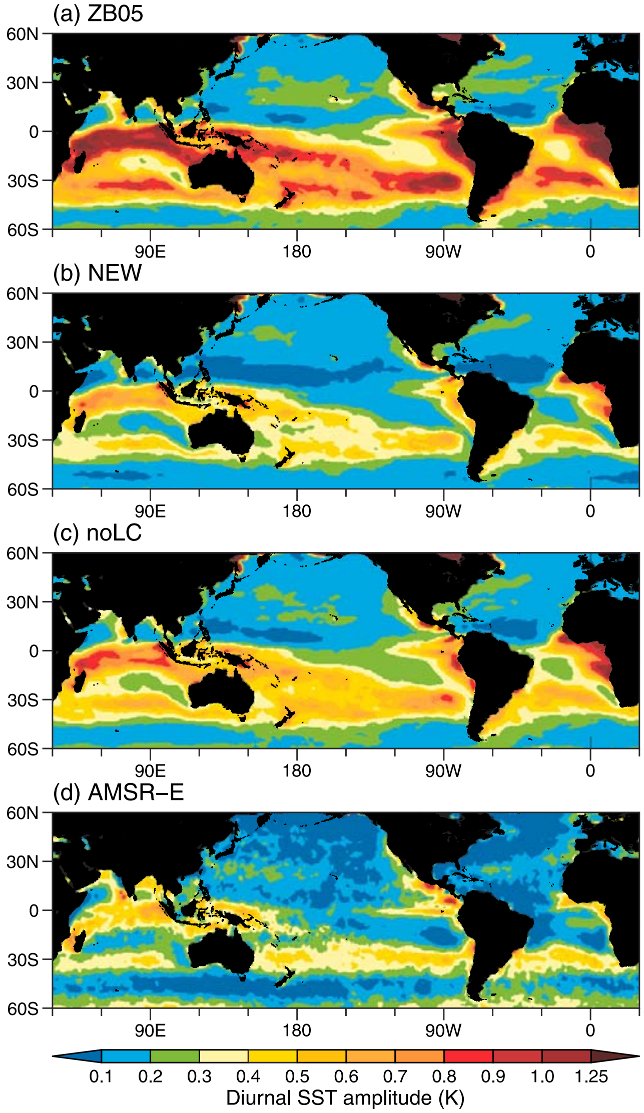

Figure 2. Spatial distributions of the mean DSA for 10 day forecast started from 1 January 1990–2007: (a) ZB05, (b) NEW, and (c) NEW without the Langmuir circulation effect. (d) Spatial distribution of the day-night difference of AMSR-E version 5 SST averaged during 2002–2006 winter [*Kawai and Wada*, 2007].

have large temperature gradients [e.g., *Gentemann et al.*, 2009]. *Gentemann et al.* [2009] found that temperature profiles observed by SkinDeEP profilers [*Ward*, 2006] show an exponential decay near the surface for wind speed of 0–1 m s^{-1}. On contrary, they reported that the temperature profiles have small gradients in the top 0.25 m as wind speed increases to 1–2 m s^{-1}. This suggests that temperature at a depth of 0.17 m can be significantly different from the skin temperature for very calm cases with wind speed about 0–1 m s^{-1}, but it is not the case for moderate to high wind conditions.

[19] Figure 5 shows results of simulations for 10 days from 28 April 1995. The time series show the simulated subskin SST and observed temperature at a depth of 0.17 m, net surface flux ($Q + R(0)$), adjusted 10 m wind speed and significant wave height computed from the ERA-Interim

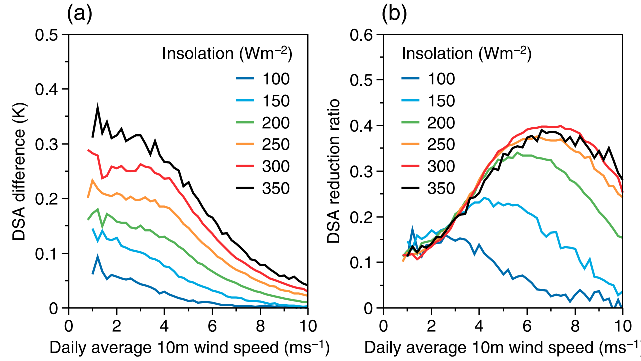

Figure 3. (a) The DSA difference between experiments with and without Langmuir circulation effect. (b) Reduction ratio of DSA due to the Langmuir circulation effect.

wave analysis. During this period, daily averaged 10 m wind speed was in a range of about 2.9 m s^{-1} to 6.6 m s^{-1}. We show 0.17 m buoy temperature as a reference since the DSA difference between 0.17 m temperature and estimated skin SST is estimated to be small (<1%) during the period except for 3 May, when the diurnal amplitude of 0.17 m temperature is about 20% smaller than that of skin SST estimated with the empirical profile of *Gentemann et al.* [2009] (please see Appendix A for the estimation method of skin SST). The ZB05 scheme simulates larger DSAs than the buoy observation for most cases. Simulated SST temperature with the modified scheme is close to the observation for weak and moderate wind conditions.

[20] Figure 6 shows the diurnal amplitudes of the simulated subskin SST with respect to those of subskin SST estimated from the buoy observation. The observed DSA of a depth of 0.17 m is corrected to the subskin DSA according to temperature profiles from *Gentemann et al.* [2009] as described in Appendix A. The diurnal amplitude is defined in the same way as section 3.1. Open and closed circles show results with the ZB05 scheme and the modified scheme, respectively. Data during the 3 month period from March to May 1995 are plotted. Data during a period from 19 to 21 April are not included because of missing values in the buoy observation. From this validation, the modified scheme shows a good agreement in the range less than 2°. For very large DSA events, the modified scheme may underestimate the DSA although the uncertainty of buoy

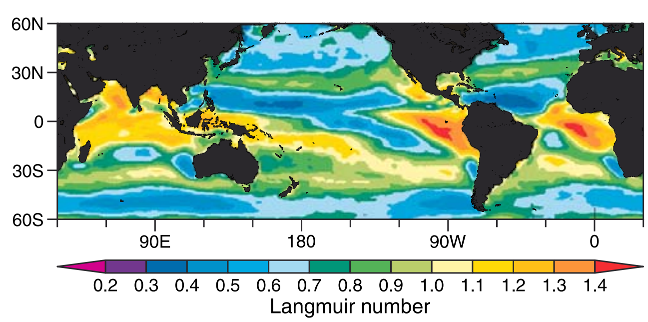

Figure 4. The average of the Langmuir number computed with forecasts starting from 1 January 1990–2007.

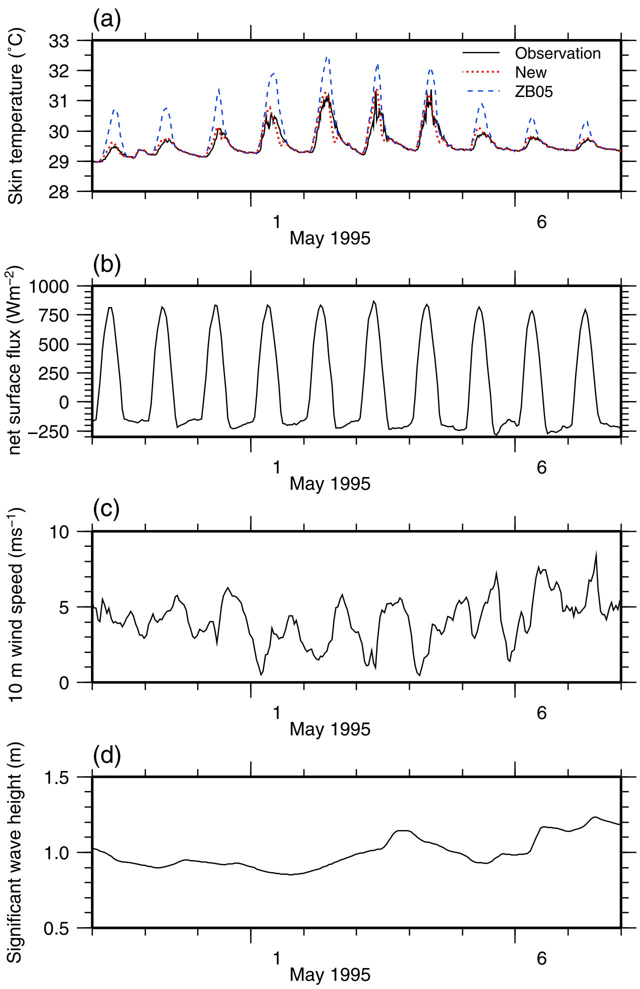

Figure 5. (a) Observed and simulated subskin SST at 15° 30′N, 61° 30′E in the Arabian Sea for 10 days from 28 April 1995. The solid line is the buoy observation at the depth of 0.17 m, the dashed line is the ZB05 scheme, and the dotted line is the modified scheme. (b) Observed net surface flux (heat and radiation fluxes). (c) The 10 m wind speed. (d) Significant wave height computed with the ERA-Interim wave analysis.

measurements and profile estimates is large at low winds. On contrary, the ZB05 scheme matches well in large DSA events (>3 K). These characteristics can be found in very calm conditions (<1 m s^{-1}) in Figures 1a and 1b. Although there is difficulty in validating DSAs with the buoy observation due to the uncertainty in the estimated DSAs in very calm conditions, it would be fair to conclude that the modified scheme reproduce well the DSA at least for small and moderate DSA ranges. For the 3 month simulations in the Arabian Sea, the root mean square errors (RMSEs) of the DSA with the modified scheme and the ZB05 scheme are 0.28 K and 1.04 K, respectively. It should be noted that the RMSEs are affected by large DSA events (>3 K), in which cases the uncertainty of the DSA estimates is large. The results from these off-line simulations are consistent with the comparison shown in Figure 1. The agreement between the independent verifications with the in situ observations and the satellite observations supports validity of the diagnostic with the empirical diurnal SST model derived from the TMI satellite measurement [*Gentemann et al.*, 2003].

4. Discussions

[21] *Bellenger and Duvel* [2009] speculated that the DSA error in the ZB05 scheme is attributed to the fixed and sharp temperature profile. However, we showed the more reliable form of the similarity function and the wave effect improve the DSA response. Therefore the error seen in the ZB05 scheme may be at least partly attributed to the improper similarity function in strongly stable conditions. The diagnostics with the TMI satellite estimate and off-line simulation with the buoy data indicate that the modified scheme may have an underestimation of the DSA for very calm and clear sky conditions. In such conditions, the stratification is prominent in upper 0.5 m. In order to reproduce the DSA of these events, the temperature profile may need to be considered in parameterizations [*Gentemann et al.*, 2009]. On the other hand, under high wind conditions the ocean mixing is intensified, so the steep profile assumed in the ZB05 scheme is not applicable [*Gentemann et al.*, 2009]. The modified scheme still has an error in moderate to high wind conditions. These errors may be attributed to an inappropriate assumption of the vertical profile for high wind conditions and omission of the wave breaking effect.

[22] Other processes such as dependency of radiant heating on chlorophyll concentration [*Ohlmann*, 2003], mixing enhancement due to wave breaking [e.g., *Gerbi et al.*, 2009; *Craig and Banner*, 1994] may improve skin layer models. None of the currently proposed skin layer models consider

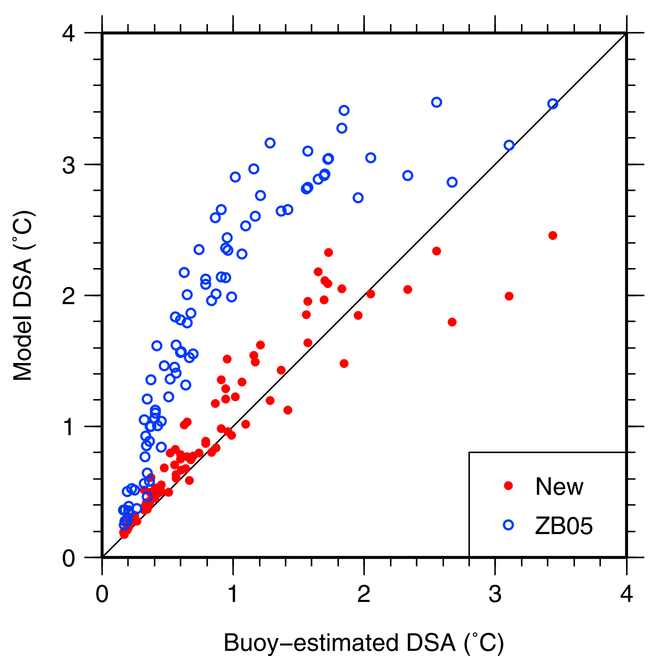

Figure 6. Diurnal amplitudes of simulated subskin SST with respect to those of subskin SST estimated with the buoy temperature observation (0.17 m) at 15° 30′N, 61° 30′E in the Arabian Sea from March to May 1995. Open and closed circles show results with the ZB05 scheme and the modified scheme, respectively.

all these processes. Further developments to include these processes are needed to yield a better representation of the diurnal skin SST variation.

[23] The parameterization of the effect of the Langmuir circulation applied in this study is based on results from LESs and the analysis of the turbulent kinetic energy (TKE) budget. In the sense of the TKE budget, the parameterization expresses TKE production by the shear of the Stokes drift velocity [*Grant and Belcher*, 2009]. Results from idealized LESs support enhanced mixing in a wide range of realistic oceanic conditions [e.g., *Li et al.*, 2005]. Therefore, we think this process exists in real situations, and makes mixing in the oceanic boundary layer different from that in the atmospheric boundary layer. Furthermore, the simulation results with the Langmuir circulation effect improved the DSA response (Figure 1) and the geographical distribution of the DSA (Figure 2) in the ECMWF model. However, from the observational point of view, it is still unclear how important the role of ocean waves for the near-surface mixing and the diurnal cycle of SST is, since it is difficult to measure and distinguish contributions of turbulent mixing from the Langmuir circulation and wave breaking. More effort to understand these processes by observations and numerical simulations is needed to improve the parameterization of these wave effects.

[24] The modified scheme shows better overall performance in terms of the DSA, particularly because moderate and small diurnal events that occur much more frequently than the very large diurnal warming events [*Bellenger and Duvel*, 2009]. The validations with the satellite data and buoy observation data demonstrate that the modified scheme reduces the mean bias in these conditions. Therefore we believe that the modified scheme is more beneficial for numerical weather prediction models.

[25] We made an attempt to validate the DSA with the off-line simulations using the buoy observations in this study. However we noticed that there is a large uncertainty in the DSA estimate in our approach related to the empirical temperature profile. In addition to the uncertainty of temperature profiles, there is observational difficulty associated with a so-called "platform effect" [*Kawai et al.*, 2006]. *Kawai et al.* [2006] investigated discrepancies of observed temperatures among TRITON buoy measurements at a depth of 0.3 m, "Sea snake" measurements in the top several centimeters and in situ radiometric measurements. They found that the radiometric skin temperature is close to 0.3 m buoy temperature even for large diurnal warming events with DSAs of 2–3°. Although their results indicate that the near-surface diurnal thermal stratification is not destroyed by the buoy hull in their observation, the accuracy of the near-surface temperature measurements from moored buoys still remains unclear. Therefore, further comprehensive validations with in situ radiometric observations like M-AERI [*Gentemann et al.*, 2009] and CIRIMS [*Jessup and Branch*, 2008] measurements and satellite observations are desirable to assess the performance of skin layer schemes for very large diurnal warming events.

5. Summary

[26] In this study, refinements to the ZB05 scheme were presented and validated. The refinements of the Monin-Obukhov similarity function for stable conditions and the mixing enhancement by the Langmuir circulation improve the diurnal SST amplitude compared with the estimate from TMI satellite measurements [*Gentemann et al.*, 2003]. The spatial distributions of the DSA with the modified scheme were compared with the AMSR-E SST observation. The modified scheme matches the observations better than the original ZB05 scheme.

[27] In addition, simulations with the buoy observations of the Arabian Sea Mixed Layer Dynamics Experiment in 1995 were performed. The model was driven by the observed surface fluxes from the IMET observations and the in situ temperature measured by the WHOI buoy. The diurnal amplitudes of simulated subskin SST was compared with those of the subskin temperature estimated from the WHOI buoy measurements at a depth of 0.17 m. The simulated subskin SST with the modified scheme shows better agreement to the buoy temperature observation than the original ZB05 scheme for small and moderate warming events. The verifications implies that the modified scheme has an underestimation of the DSA for very large DSA events, although the uncertainty is still a big issue in the verification for very large DSA events. Overall these results confirm the better performance of the modified scheme and support validity of the diagnostic with the empirical diurnal SST model derived from the TMI satellite measurement.

[28] It was found that the parameterization of the Langmuir circulation (the Stokes drift) effect enhances ocean mixing near the surface and reduces the diurnal SST amplitude under wavy conditions. This result implies that ocean wave processes have a significant impact on the diurnal SST variability and that the wave effects need to be taken into account in upper ocean models. Numerical weather prediction models may be improved with more sophisticated parameterizations of upper ocean processes with coupling to ocean wave models.

Appendix A: Assessment of Skin SST With the Buoy Observed SST

[29] Skin SST is assessed with the buoy temperature measurements at a depth of 0.17 m, since the in situ radiometric skin SST measurements are unavailable in the Arabian Sea Mixed Layer Dynamics Experiment. The DSAs at 0.17 m for very calm conditions are smaller than that of skin temperature in calm and clear sky conditions. Although it is difficult to assess large DSA events without in situ radiometric observations, here we try to estimate skin SST with observed 0.17 m temperature.

[30] Recently *Gentemann et al.* [2009] has investigated near-surface temperature profiles observed from SkinDeEP measurements [*Ward et al.*, 2004]. They developed an empirical formula of temperature profiles on the basis of wind speed and warm layer depth. The formula is given by equation 17 of *Gentemann et al.* [2009] as

$$\Delta T(z) = e^{-9.5\left(\frac{z}{D}\right)^{a}}, \tag{A1}$$

where ΔT is a temperature profile normalized by skin SST, z is a depth, D is a warm layer depth and a is a parameter depends on wind speed. The parameter a increases from 2 to 9 as wind speed increases [see *Gentemann et al.*, 2009, Table 1]. The temperature profile has steep gradient near the surface in calm conditions (<1.5 m s^{-1}), on the other hand, the temperature gradient vanishes in moderate and high wind conditions. It is impossible to estimate the warm layer depth from the buoy observation data for large DSA events, because the warm layer depth becomes less than 1 m. So, the warm layer depth is estimated with the procedure of the *Fairall et al.*'s [1996a] scheme. It should be noted that the temperature profile is sensitive to the estimated warm layer depth, so the estimated profile is prone to have errors associated with this uncertainty. Once wind speed and the estimated warm layer depth are given, the diurnal amplitudes of subskin temperature are corrected by using the ratio of the DSA between the subskin temperature and the buoy temperature at 0.17 m.

[31] **Acknowledgments.** We would like to thank Yoshimi Kawai at the Japan Agency for Marine-Earth Science and Technology and Akiyoshi Wada at the Meteorological Research Institute who kindly provided AMSR-E SST data for reproduction. We also would like to thank the Woods Hole Oceanographic Institution for making available the buoy observations, which were invaluable in this model development.

References

Baumgartner, M. F., N. J. Brink, W. M. Ostrom, R. P. Trask, and R. A. Weller (1997), Arabian Sea Mixed Layer Dynamics Experiment data report, *Tech. Rep. WHOI-97-08*, 157 pp., Woods Hole Oceanogr. Inst., Woods Hole, Mass.

Bellenger, H., and J.-P. Duvel (2009), An analysis of tropical ocean diurnal warm layers, *J. Clim.*, *22*, 3629–3646.

Brunke, M. A., X. Zeng, V. Misra, and A. Beljaars (2008), Integration of a prognostic sea surface skin temperature scheme into weather and climate models, *J. Geophys. Res.*, *113*, D21117, doi:10.1029/2008JD010607.

Cheng, Y., and W. Brutsaert (2005), Flux-profile relationships for wind speed and temperature in the stable atmospheric boundary layer, *Boundary Layer Meteorol.*, *114*(3), 519–538.

Craig, P. D., and M. L. Banner (1994), Modeling wave-enhanced turbulence in the ocean surface layer, *J. Phys. Oceanogr.*, *24*, 2546–2559.

Donlon, C., et al. (2007), The global ocean data assimilation experiment high-resolution sea surface temperature pilot project, *Bull. Am. Meteorol. Soc.*, *88*(8), 1197–1213.

Fairall, C. W., E. F. Bradley, J. S. Godfrey, G. A. Wick, J. B. Edson, and G. S. Young (1996a), Cool-skin and warm-layer effects on sea surface temperature, *J. Geophys. Res.*, *101*(C1), 1295–1308.

Fairall, C. W., E. F. Bradley, D. P. Rogers, J. B. Edson, and G. S. Young (1996b), Bulk parameterization of air-sea fluxes for Tropical Ocean-Global Atmosphere Coupled-Ocean Atmosphere Response Experiment, *J. Geophys. Res.*, *101*(C2), 3747–3764.

Gentemann, C. L., and P. J. Minnett (2008), Radiometric measurements of ocean surface thermal variability, *J. Geophys. Res.*, *113*, C08017, doi:10.1029/2007JC004540.

Gentemann, C. L., C. J. Donlon, A. Stuart-Menteth, and F. J. Wentz (2003), Diurnal signals in satellite sea surface temperature measurements, *Geophys. Res. Lett.*, *30*(3), 1140, doi:10.1029/2002GL016291.

Gentemann, C. L., P. J. Minnett, and B. Ward (2009), Profiles of ocean surface heating (POSH): A new model of upper ocean diurnal warming, *J. Geophys. Res.*, *114*, C07017, doi:10.1029/2008JC004825.

Gerbi, G. P., J. H. Trowbridge, J. B. Edson, A. J. Plueddemann, E. A. Terray, and J. J. Fredericks (2008), Measurements of momentum and heat transfer across the air-sea interface, *J. Phys. Oceanogr.*, *38*, 1054–1072.

Gerbi, G. P., J. H. Trowbridge, E. A. Terray, A. J. Plueddemann, and T. Kukulka (2009), Observations of turbulence in the ocean surface boundary layer: Energetics and transport, *J. Phys. Oceanogr.*, *39*, 1077–1096.

Grachev, A. A., E. L Andreas, C. W. Fairall, P. S. Guest, and P. O. G. Persson (2007), SHEBA flux-profile relationships in the stable atmospheric boundary layer, *Boundary Layer Meteorol.*, *124*, 315–333.

Grant, A. L. M., and S. E. Belcher (2009), Characteristics of Langmuir turbulence in the ocean mixed layer, *J. Phys. Oceanogr.*, *39*, 1871–1887.

Janssen, P. (2004), *The Interaction of Ocean Waves and Wind*, 300 pp., Cambridge Univ. Press, Cambridge, U. K.

Jessup, A. T., and R. Branch (2008), Integrated ocean skin and bulk temperature measurements using the Calibrated Infrared In Situ Measurement System (CIRIMS) and through-hull ports, *J. Atmos. Oceanic Technol.*, *25*, 579–597.

Kawai, Y., and A. Wada (2007), Diurnal sea surface temperature variation and its impact on the atmosphere and ocean: A review, *J. Oceanogr.*, *63*, 721–744.

Kawai, Y., H. Kawamura, S. Tanba, K. Ando, K. Yoneyama, and N. Nagahama (2006), Validity of sea surface temperature observed with the TRITON buoy under diurnal heating conditions, *J. Oceanogr.*, *62*, 825–838.

Kenyon, K. E. (1969), Stokes drift for random gravity waves, *J. Geophys. Res.*, *74*(28), 6991–6994.

Langmuir, I. (1938), Surface motion of water induced by wind, *Science*, *87*, 119–123.

Large, W. G., J. C. McWilliams, and S. C. Doney (1994), Oceanic vertical mixing: A review and a model with a nonlocal boundary layer parameterization, *Rev. Geophys.*, *32*, 363–403.

Li, M., C. Garrett, and E. Skyllingstad (2005), A regime diagram for classifying turbulent large eddies in the upper ocean, *Deep Sea Res. Part I*, *52*, 259–278.

Madden, R. A., and P. R. Julian (1994), Observation of the 40–50 day tropical oscillation: A review, *Mon. Weather Rev.*, *122*, 814–837.

McWilliams, J. C., and P. P. Sullivan (2000), Vertical mixing by Langmuir circulations, *Spill Sci. Technol. Bull.*, *6*, 225–237.

McWilliams, J. C., P. P. Sullivan, and C.-H. Moeng (1997), Langmuir turbulence in the ocean, *J. Fluid Mech.*, *334*, 1–30.

Melville, W. K. (1996), The role of surface-wave breaking in air-sea interaction, *Annu. Rev. Fluid Mech.*, *28*, 279–321.

Noh, Y., H. S. Min, and S. Raasch (2004), Large eddy simulation of the ocean mixed layer: The effects of wave breaking and Langmuir circulation, *J. Phys. Oceanogr.*, *34*, 720–735.

Ohlmann, J. C. (2003), Ocean radiant heating in climate models, *J. Clim.*, *16*, 1337–1351.

Simmons, A., S. Uppala, D. Dee, and S. Kobayashi (2007), ERA-Interim: New ECMWF reanalysis products from 1989 onwards, in *ECMWF Newsletter*, vol. 110, pp. 25–35, Eur. Cent. for Medium-Range Weather Forecasts, Reading, U. K. (Available at http://www.ecmwf.int/publications/newsletters.)

Skyllingstad, E. D., and D. W. Denbo (1995), An ocean large-eddy simulation of Langmuir circulations and convection in the surface mixed layer, *J. Geophys. Res.*, *100*(C5), 8501–8522.

Smyth, W. D., E. D. Skyllingstad, G. B. Crawford, and H. Wijesekera (2002), Nonlocal fluxes and Stokes drift effects in the K-profile parameterization, *Ocean Dyn.*, *52*(3), 104–115.

Soloviev, A. V. (1982), On the vertical structure of the ocean thin surface layer at light wind, *Dokl. Acad. Sci. USSR Earth Sci. Sect. Engl. Transl.*, *18*, 751–760.

Stuart-Menteth, A. C., I. S. Robinson, and P. G. Challenor (2003), A global study of diurnal warming using satellite-derived sea surface temperature, *J. Geophys. Res.*, *108*(C5), 3155, doi:10.1029/2002JC001534.

Sullivan, P. P., and J. C. McWilliams (2010), Dynamics of winds and currents coupled to surface waves, *Annu. Rev. Fluid Mech.*, *42*, 19–42.

Sullivan, P. P., J. C. McWilliams, and W. K. Melville (2007), Surface gravity wave effects in the oceanic boundary layer: Large-eddy simulation with vortex force and stochastic breakers, *J. Fluid Mech.*, *593*, 405–452.

Terray, E. A., M. A. Donelan, Y. C. Agrawal, W. M. Drennan, K. K. Kahma, A. J. Williams III, P. A. Hwang, and S. A. Kitaigorodskii (1996), Estimates of kinetic energy dissipation under breaking waves, *J. Phys. Oceanogr.*, *26*, 792–807.

Thorpe, S. A. (2004), Langmuir circulation, *Annu. Rev. Fluid Mech.*, *36*, 55–79.

Thorpe, S. A., T. R. Osborn, J. F. E. Jackson, A. J. Hall, and R. G. Lueck (2003), Measurements of turbulence in the upper-ocean mixing layer using autosub, *J. Phys. Oceanogr.*, *33*, 122–145.

Ward, B. (2006), Near-surface ocean temperature, *J. Geophys. Res.*, *111*, C02004, doi:10.1029/2004JC002689.

Ward, B., R. Wanninkhof, P. J. Minnett, and M. J. Head (2004), SkinDeEP: A profiling instrument for upper-decameter sea surface measurements, *J. Atmos. Oceanic Technol.*, *21*, 207–222.

Webster, P. J., C. A. Clayson, and J. A. Curry (1996), Clouds, radiation, and the diurnal cycle of sea surface temperature in the tropical western Pacific, *J. Clim.*, *9*, 1712–1730.

Weller, R. A., A. S. Fischer, D. L. Rudnick, C. C. Eriksen, T. D. Dickey, J. Marra, C. Fox, and R. Leben (2002), Moored observations of upper-ocean response to the monsoons in the Arabian Sea during 1994–1995, *Deep Sea Res. Part II*, *49*, 2195–2230.

Zeng, X., and A. Beljaars (2005), A prognostic scheme of sea surface skin temperature for modeling and data assimilation, *Geophys. Res. Lett.*, *32*, L14605, doi:10.1029/2005GL023030.

A. C. M. Beljaars, J.-R. Bidlot, P. A. E. M. Janssen, and Y. Takaya, European Centre for Medium-Range Weather Forecasts, Shinfield Park, Reading RG2 9AX, UK. (anton.beljaars@ecmwf.int; jean.bidlot@ecmwf.int; peter.janssen@ecmwf.int; yuhei.takaya@ecmwf.int)